The fragility of Al–Ni-based glass-forming melts

2003 J. Phys.: Condens. Matter 15 5409

(http://iopscience.iop.org/0953-8984/15/32/302)

INSTITUTE OF PHYSICS PUBLISHING JOURNAL OF PHYSICS: CONDENSED MATTER

J. Phys.: Condens. Matter **15** (2003) 5409–5415 PII: S0953-8984(03)58913-5

The fragility of Al–Ni-based glass-forming melts

Pengchao Si[1], Xiufang Bian, Junyan Zhang, Hui Li, Minhua Sun and Yan Zhao

Key Laboratory of Liquid Structure and Heredity of Materials, Education Ministry of China, Shandong University (South campus), Jingshi Road 73, Jinan 250061, People's Republic of China

E-mail: PCSi@sdu.edu.cn

Received 29 January 2003, in final form 27 May 2003
Published 1 August 2003
Online at stacks.iop.org/JPhysCM/15/5409

Abstract

In the original description of fragility, Angell (1988 *J. Phys. Chem. Solids* **49** 863) determined the degree of fragility from the curvature on an Arrhenius plot. This paper discusses a new measurement of the fragility value. The fragility of Al–Ni-based glass-forming melts, which is seldom reported in this field, can be analysed by using data from their viscosity and thermal properties. The fragility is observed to be very high, which is in very good agreement with the low glass-forming ability of Al–Ni-based alloys.

1. Introduction

Since being described originally by Angell [1], the concept of fragility is now widely used to classify glass-forming liquids. Fragile liquids are so named because their configurational structures have a rapid breakdown with increasing temperature close to the glass transition temperature, T_g. But the configurational structures of strong liquids do not change much with temperature [2, 3]. The degree of fragility relates the temperature dependence of the viscosity of the supercooled liquid to its thermodynamic properties [4]. A lot of data from research reveals that there is a close relationship between fragility and viscosity. Viscosity is also an important physical property of liquid metals. From the microscopic point of view, the most characteristic feature of a liquid results from the high mobility of its individual atoms. However, the motions of atoms through a liquid are impeded by the frictional forces set up by their nearest neighbours. Consequently, the viscosity of a liquid is of great interest in both the technology and theory of liquid metal behaviour. But viscosity data is available for just a limited number of metallic glasses [5]. Busch and co-workers [6] performed some viscosity measurements on these metallic glasses by using parallel-plate rheometry and three-point beam bending. Both methods require bulk samples [6]. However, Al-based alloys are almost impossible to obtain as bulk metallic glasses (BMGs). Until now, the largest thickness of Al-based glass was only about 300 μm [7].

[1] Author to whom any correspondence should be addressed.

0953-8984/03/325409+07$30.00

In our work, we measured the viscosity of the Al–Ni-based alloy melts at high temperature and calculated the value of m, the factor of fragility. The main purpose of this paper is to discuss the relationship between viscosity and the ability of Al–Ni-based alloys to form glasses, which might be helpful in understanding the structure of the Al–Ni-based metal glass and in obtaining Al-based BMGs.

2. Method

All equilibrium viscosity data obtained in the melt can be described very well by the Arrhenius equation

$$\eta = \eta_0 \exp\left[\frac{E_a}{RT}\right] \tag{1}$$

where E_a is an activation energy and R is the gas constant. So, by using equation (1), the parameters E_a and η_0 can be calculated from the data for $\eta(T)$ (where $\eta(T)$ is obtained using a torsional oscillation viscometer for high temperature). Meanwhile, the equilibrium viscosity data, which are obtained in the supercooled liquid, can be fitted very well using the Vogel–Fulcher–Tammann (VFT) relation [6]:

$$\eta = \eta_0 \exp\left[\frac{B}{T - T_0}\right] \tag{2}$$

where η_0, B and T_0 are fitting parameters and T is the temperature.

It has not been reported that, in the present reports, there are phase transitions from the liquid to the supercooled liquid. But there is no inflexion on the viscosity–temperature curve during this process. So, it is believed that the Arrhenius equation (1) and the VFT equation (2) are both fitted at the transition temperature, T_m. Then

$$\eta_1(T_m) = \eta_2(T_m) \tag{3}$$

$$\left.\frac{d(\eta 1)}{dT}\right|_{T_m} = \left.\frac{d(\eta 2)}{dT}\right|_{T_m} \tag{4}$$

where η_1 is obtained from equation (1) and η_2 is obtained from equation (2).

Also, the glass transition temperature is the value at which the equilibrium liquid has a viscosity of 10^{12} Pa s [8, 9]. What's more, the VFT fits can be extrapolated to determine the temperature corresponding to $\eta = 10^{12}$ Pa s. So, combining equations (2) and (3), the parameters B and T_0 can be calculated from the data $\eta(T_m)$ and $\eta(T_g)$ (here $\eta(T_g) = 10^{12}$ Pa s).

To quantify the fragility, Böhmer and his co-workers [10] introduced a fragility parameter m, defined as

$$m = \left.\frac{d \log_{10} \tau(T)}{d(T_g/T)}\right|_{T=T_g} \tag{5}$$

where $\tau(T)$ is a characteristic temperature-dependent relaxation time. Since the viscosity is proportional to a structural relaxation time, m can be estimated by replacing $\tau(T)$ with $\eta(T)$ in equation (5). Then

$$m = \left.\frac{\partial \log \eta(T)}{\partial(T_g/T)}\right|_{T=T_g} = \frac{BT_g}{(T_g - T_0)^2 \ln(10)}. \tag{6}$$

Usually, $m \geqslant 100$ for fragile liquids. However, the value of m for strong liquids is often between 16 and 30 [10]. For metallic glasses, such as Zr-based and Pd-based amorphous alloys, m has values in the range from 32 to 66 [11].

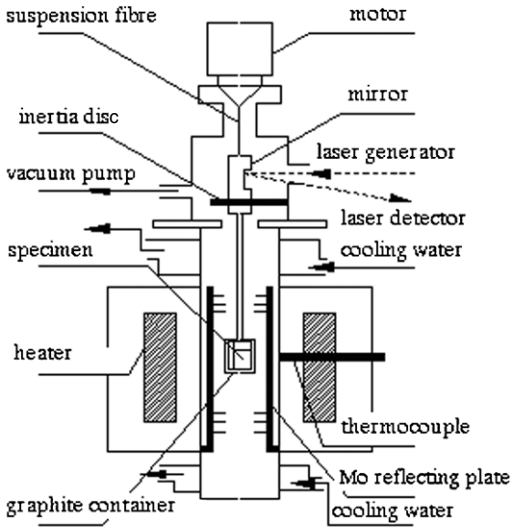

Figure 1. A schematic diagram of a torsional oscillation viscometer.

Table 1. The related parameters of amorphous $Al_{90}Ni_5Ce_5$, $Al_{85}Ni_{10}Ce_5$, $Al_{84}Ni_{10}La_3Ce_3$ and $Al_{80}Ni_{15}Ce_5$ alloys. (Note that: T_g, T_x and T_m are the glass transition, on-set crystallization and melting temperatures, respectively; η_0, B and T_0 are fitting constants for the VFT equation (2); E_a is an activation energy and R is the gas constant of the Arrhenius equation (1); m_x is the fragility index; and v_0 is the lowest circumferential speed to obtain amorphous ribbons.)

	v_0 (m s^{-1})	T_g (K)	T_x (K)	T_m (K)	η_0 (10^{-3} Pa s)	T_0 (K)	E_a/R (K)	B (K)	m_x
$Al_{90}Ni_5Ce_5$	22	—	605	890	0.199 38	566	2261	1328	229
$Al_{85}Ni_{10}Ce_5$	11	519	537	889	0.240 31	505	2691	1164	265
$Al_{84}Ni_{10}La_3Ce_3$	5.5	—	504	889	0.447 85	481	1744	800	331
$Al_{80}Ni_{15}Ce_5$	33	—	641	887	0.249 16	576	2908	1020	67

3. Experimental details

The samples of Al-based alloys used in this work were prepared from pure ingot Al (99.9% mass), pure ingot Ni (99.9% mass), pure ingot La (99.6% mass) and pure ingot Ce (99.9% mass). The purity is sufficient for this experiment.

Using a single roller melt-spinning apparatus, the pre-alloyed ingots were re-melted by high-frequency induction heating and rapidly solidified into continuous ribbons at different circumferential speeds (v_0—see table 1) in a controlled inert (argon) atmosphere. The ribbons were about 20–40 μm in thickness and 4–6 mm in width. The thermal properties of the melt-spinning ribbons were investigated using a Netzsch DSC404 calorimeter with standards of pure indium (99.999% mass) and zinc (99.999% mass).

Firstly, the samples of Al–Ni-based alloys, which were sealed in a vacuum of 10^{-3} Torr, were first overheated to 1250 °C and held at this temperature for 4 h. Then the samples were cooled to the required temperature before the viscosity measurement was performed using a torsional oscillation viscometer (figure 1) for high-temperature melts. Every sample of Al–Ni-based alloy was placed in an alumina crucible. (In this work, the crucible is columniform. The aspect ratio of the crucible is as follows: the inner diameter is 28 mm; the outer diameter

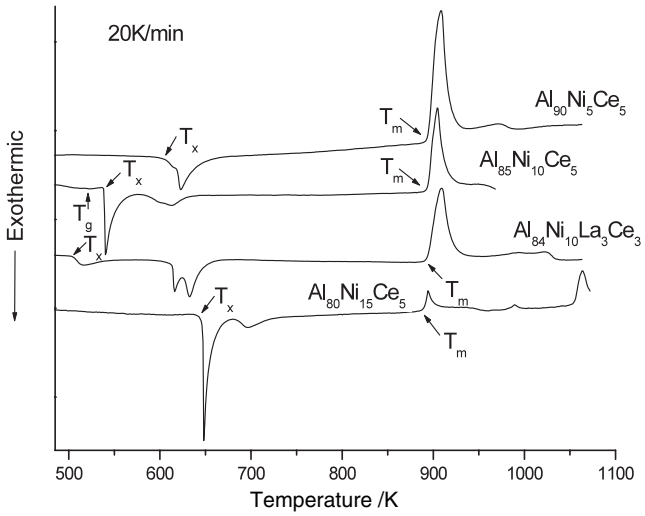

Figure 2. Differential scanning calorimetric curves of amorphous $Al_{90}Ni_5Ce_5$, $Al_{85}Ni_{10}Ce_5$, $Al_{84}Ni_{10}La_3Ce_3$ and $Al_{80}Ni_{15}Ce_5$ alloys.

is 32 mm; the height is 62 mm.) Next, the crucible was placed in a vessel hung by a torsional suspension and the vessel was set in oscillation about a vertical axis. The resulting motion was gradually damped on account of frictional energy absorption and dissipation within the melt. The viscosity of the liquid sample can be calculated using equation [12]:

$$\nu = \frac{I^2(\delta - T\delta_0/T_0)^2}{\pi(MR)^2 T W^2}. \tag{7}$$

Here

$$W = 1 - \frac{3}{2}\Delta - \frac{3}{8}\Delta^2 - a + (b - c\Delta)\frac{2nr}{H} \tag{8}$$

where $\Delta = \delta/2\pi$, M represents the mass of the liquid sample, and a, b and c are constants. I represents the moment of inertia of the suspended system, r is the radius of the vessel, H is the height of the liquid sample in the vessel, δ refers to the logarithmic damping decrement, and T is the period of the oscillations, while the subscript 0 refers to an empty vessel. n is the number of solid planes contacted horizontally by the liquid sample (i.e. in the case of a vessel having its lower end closed and its upper surface free, then $n = 1$; if the vessel encloses the fluid top and bottom, then $n = 2$). The dynamic viscosity η can be calculated using the following formula: $\eta = \nu\rho$, where ρ is the density of the sample.

4. Results

Figure 2 shows differential scanning calorimetric curves of amorphous $Al_{90}Ni_5Ce_5$, $Al_{85}Ni_{10}Ce_5$, $Al_{84}Ni_{10}La_3Ce_3$ and $Al_{80}Ni_{15}Ce_5$ (at.%) alloys at a heating rate of 20 K min^{-1} (by DSC), respectively. It shows that only $Al_{85}Ni_{10}Ce_5$ has a clear glass transition temperature, T_g (519 K). The on-set crystallization temperatures T_x and melting temperatures, respectively, of these amorphous alloys are marked on the DSC pattern. In our work, all the ribbons of amorphous alloys have been demonstrated to be fully amorphous.

From the DSC analysis, the melting temperature of the Al–Ni-based alloys is about 899 K. So the alloys are still liquid during viscosity measurements from 1100–1500 K. Different

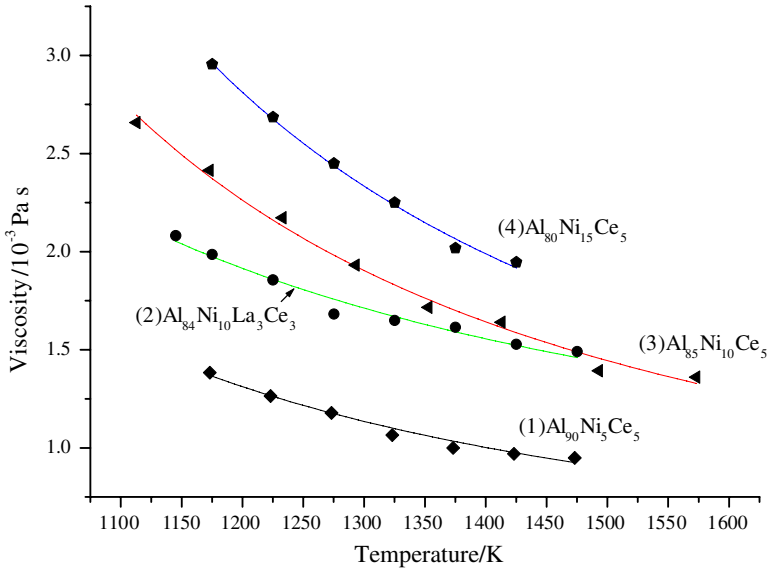

Figure 3. Different experimental viscosity data (as single points) and fitting curves (as continuous curves) for $Al_{90}Ni_5Ce_5$, $Al_{85}Ni_{10}Ce_5$, $Al_{84}Ni_{10}La_3Ce_3$ and $Al_{80}Ni_{15}Ce_5$ alloys melts.
(This figure is in colour only in the electronic version)

viscosity curves of $Al_{90}Ni_5Ce_5$, $Al_{85}Ni_{10}Ce_5$, $Al_{84}Ni_{10}La_3Ce_3$ and $Al_{80}Ni_{15}Ce_5$ liquid alloys are shown in figure 3. These curves are drawn from viscosity data obtained using a torsional oscillation viscometer for high-temperature melts. They fit the Arrhenius equation (1) well.

All related parameters are listed in table 1. It is found that only T_g (519 K) of $Al_{85}Ni_{10}Ce_5$ can be obtained clearly. All the on-set melting temperatures of Al–Ni-based amorphous alloys are close to 889 K. Unfortunately, it is hard to obtain the amorphous ribbons below v_0 in our work. It can be seen from table 1 that the value of v_0 for $Al_{84}Ni_{10}La_3Ce_3$ is the lowest.

5. Discussion

It is reported that not all the amorphous alloys have a clear T_g point in their DSC curves [13]. In the work of Inoue and co-workers [14, 15], which is on the $Nd_{60}Fe_{30}Al_{10}$ and $Pr_{60}Fe_{30}Al_{10}$ amorphous alloys, it is believed that $T_g \geqslant T_x$ corresponds to the weak thermodynamic stability of amorphous alloys. In our study, T_g could not be separated easily from T_x (figure 2), so we replace T_g with T_x in equation (6). Then the following can be adopted:

$$m_x = \left.\frac{\partial \log \eta(T)}{\partial (T_x/T)}\right|_{T=T_x} = \frac{BT_x}{(T_x - T_0)^2 \ln(10)}. \tag{9}$$

The values of m_x for $Al_{90}Ni_5Ce_5$, $Al_{85}Ni_{10}Ce_5$, $Al_{84}Ni_{10}La_3Ce_3$ and $Al_{80}Ni_{15}Ce_5$ that were calculated from the viscosity data of Al–Ni-based alloys using equation (9) are 229, 265, 331 and 67, respectively (table 1). These are much higher than the known fragility parameters of other metallic alloys [10, 11]. Generally speaking, the value of m is much larger, the liquid of the alloy is more fragile, and glass forming is more difficult [6, 11]. So, the fact that Al–Ni-based BMGs are difficult to obtain is in accord with their high fragility value compared to those of other metallic glasses. However, this law could not fit Al–Ni-based alloys considering their cooling speeds (lowest circumferential speeds) in this experiment. Among these Al–Ni-based

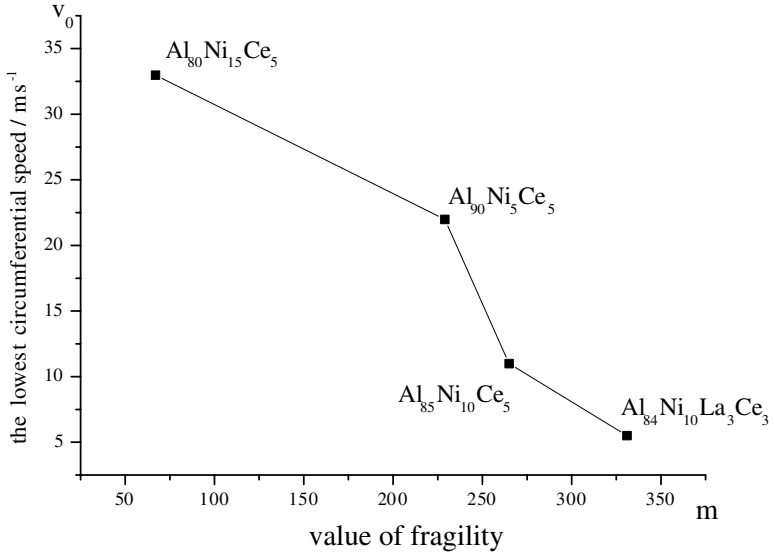

Figure 4. The relation between the value of fragility and the lowest circumferential speed.

alloys, for $Al_{84}Ni_{10}La_3Ce_3$ the value of m is the highest but the cooling rate v_0 is the lowest. In contrast, for $Al_{80}Ni_{15}Ce_5$ v_0 is the highest but m is the lowest. Figure 4 shows that the lowest circumferential speed, v_0, evidently decreases as the value of fragility, m, increases. It is known that the cooling speed has an important influence on the formation of metallic glass. When v_0 is low, the ability to form metallic glass is high. So, a liquid of $Al_{84}Ni_{10}La_3Ce_3$ should form an amorphous alloy more easily than that of $Al_{80}Ni_{15}Ce_5$. This is inconsistent with the law on fragility. This result is unexpected since, for Zr-rich glasses, Busch and co-workers [16] reported that the less fragile glass-forming alloys are kinetically more stable. In other words, this is abnormal for Al–Ni-based alloys.

Recently, Gerhard Wilde found that, for two Pd-based BMGs $Pd_{40}Ni_{40}P_{20}$ and $Pd_{43}Cu_{27}Ni_{10}P_{20}$, fragility and thermal stability are not necessarily coupled [17]. Only under growth-controlled vitrification conditions, when a high melt viscosity prevents rapid growth after initial nucleation, does the law on fragility apply. During nucleation-controlled vitrification, where nucleation is avoided, the higher kinetic ability against crystallization is not always in agreement with the lower value of fragility. In our work, the values of m_x for $Al_{84}Ni_{10}La_3Ce_3$ and $Al_{80}Ni_{15}Ce_5$ glass-forming melts are 331 and 67, respectively. However, amorphous $Al_{84}Ni_{10}La_3Ce_3$ alloy could be obtained more easily than amorphous $Al_{80}Ni_{15}Ce_5$ alloy from their melts, although its fragility value is the highest. This fact does not accord with the law on fragility. In contrast to the Zr-rich BMG, our results indicate clearly that vitrification of the Al–Ni-based systems is nucleation-controlled.

6. Conclusions

From the viscosity data of Al–Ni-based alloy melts at high temperature and also from the thermal properties, the fragility parameters, m, for Al–Ni-based alloy liquids have been calculated. The values of m are much higher than those for other metallic glasses. This is consistent with their low glass-forming ability. But in Al–Ni-based alloys systems, the

liquid of $Al_{84}Ni_{10}La_3Ce_3$ can form an amorphous alloy most easily, which is not agreement with its highest fragility value. The abnormal properties of Al–Ni-based alloys are due to the fact that vitrification of the Al–Ni-based alloys systems is nucleation-controlled.

Acknowledgments

The authors are grateful for the support of the National Natural Science Foundation of the People's Republic of China and the Natural Science Foundation of Shandong Province, China, under grants 50231040 and Z2001F02, respectively.

References

[1] Angell C A 1988 *J. Phys. Chem. Solids* **49** 863
[2] Angell C A 1985 *Relaxation in Complex Systems* ed K Ngai and G B Wright (Springfield, VA: National Technical Information Service, US Department of Commerce) p 3
[3] Hodge I M 1996 *J. Non-Cryst. Solids* **202** 164
[4] Brüning R and Sutton M 1996 *J. Non-Cryst. Solids* **205–207** 480
[5] Chen H S 1978 *J. Non-Cryst. Solids* **27** 257
[6] Busch R, Bakke E and Johnson W L 1998 *Acta Mater.* **46** 4725
[7] Bian X F and Sun M H 2003 *Mater. Lett.* **57** 2460
[8] Laughin W T and Uhlmann D R 1972 *J. Phys. Chem.* **76** 2371
[9] Angell C A 1995 *Science* **267** 1924
[10] Böhmer R, Ngai K L, Angell C A and Plazek D J 1993 *J. Chem. Phys.* **99** 4201
[11] Perera D N 1999 *J. Phys.: Condens. Matter* **11** 3807
[12] Emadi D, Gruzleski J E and Toguri J M 1993 *Metal. Trans.* B **24** 1055
[13] Inoue A 1998 *Prog. Mater. Sci.* **43** 365
[14] Inoue A, Zhang T and Takeuchi A 1996 *J. Mater. Trans. JIM* **37** 1731
[15] Inoue A *et al* 1996 *J. Mater. Trans. JIM* **37** 636
[16] Busch R, Masuhr A, Bakke E and Johnson W L 1997 *Mater. Res. Soc. Symp. Proc.* **455** 369
[17] Wilde G 2002 *J. Non-Cryst. Solids* **312–314** 537